Nanohydroxy Apatite/Activated Carbon as Supported Liquid Membrane for Fission Products

A.T. Kassem, N. El-said, H, F. Aly

Abstract- The study of permeability of ^{137}Cs, ^{90}Sr and ^{60}Co from nitrate media was carried out using Nanocomposite hydroxy apatite/activated carbon. The efficiency of this extractant was studied under various experimental conditions, such as aqueous pH,$NaNO_3$M present in the initial aqueous feed , Nanocomposite hydroxy apatite as carrier in the membrane disc ,EDTA as stripping phase concentration, temperature and time of extraction were studied The percentage of ^{137}Cs, ^{90}Sr and ^{60}Co extraction decreases with the increase of temperature at varying concentration of Nanocomposite hydroxy apatite. The pertraction of ^{137}Cs, ^{90}Sr and ^{60}Co from nitrate media were examined at the optimized conditions. Under the optimum experimental conditions 98.6–99.9% of ^{137}Cs was extracted in 10–30 min with the initial feed concentration of 0.5 $NaNO_3$ This Study was developed using a new nanohydroxyapatite–Activated carbon. The nanohydroxyapatite (nHAP) particles mixed with Activated Carbon (AC) acts as the inorganic phase was mixed with activated carbon (AC) forming HAp-AC composite. Facilitated transport supported liquid membranes (SLMs) were prepared at 20°C temperature. Recently novel compositions in this system HAp-AC were described and characterized with regard to DTA,SEM, IR ,surface investigated and spectra. The process of diffusion in liquid membranes is governed by chemical diffusion process .Fick's first law of diffusion.

Keywords- NHAP: -AC, -AC, DTA,SEM, IR ,surface investigated and spectra.

I. INTRODUCTION

The removal of radioactive isotopes (such as $^{152+154}Eu$, ^{137}Cs, ^{90}Sr and ^{60}Co was investigated by using hydroxyapatite, an effective inorganic sorbent, at the ultrafine particle size range. In bench-scale experiments performed batch wise, the influence of the main sorption parameters were examined (i.e., solution pH, sorbent and Hydroxyapatite (HAp) is often used as a bone implant material because it is biocompatible and osteoconductive. However, HAp possesses poor rheological properties and it is inactive against disease-causing microbes. To improve these properties, we developed a green method to synthesize multifunctional composites containing: (1) cellulose (CEL) to impart mechanical strength; (2) chitosan (Eu) to induce antibacterial activity thereby maintaining a microbe free wound site; and (3) HAp. In this method, Cs and CEL[CELCs] were co-dissolved in an ionic liquid (IL) and then regenerated from water. HAp was subsequently formed in situ by alternately soaking [CELEu] composites in aqueous solutions of $CaCl_2$ and Na_2HPO_4. At least 88% of IL used was recovered for reuse by distilling the aqueous washings of [CELEu]. The composites were characterized using FTIR, XRD, and SEM.

Revised Version Manuscript Received on June 05, 2015.

A. T. Kassem, Hot Labs. And Waste Management Center, Atomic, Energy Authority, P.C. 13759, Cairo, Egypt.
N. El-Said, Hot Labs. And Waste Management Center, Atomic, Energy Authority, P.C. 13759, Cairo, Egypt.
H, F. Aly, Hot Labs. And Waste Management Center, Atomic, Energy Authority, P.C. 13759, Cairo, Egypt.

These composites retained the desirable properties of their constituents. For example, the tensile strength of the composites was enhanced 1.9 times by increasing CEL loading from 20% to 80%. Incorporating Eu in the composites resulted in composites which inhibited the growth of both Gram positive (MRSA, S. aureus and VRE) and Gram negative (E. coli and P. aeruginosa) bacteria. These findings highlight the potential use of [CELCSHAp] composites as scaffolds in bone tissue engineering. VC 2013 Wiley Periodicals, Hydroxyapatite (HAp), the main component of teeth and bones has received considerable attention as suitable material for bone tissue engineering because it is both biocompatible and osteoconductive.1,2 Despite these excellent properties, 10 and 20 min, preceded by rinsing with either distilled deionized water, Liquid wastes create the greatest problems with regard to both processing and waste disposal. One of the most radionuclides are produced are cobalt(^{60}Co) in high level waste as corrosion products[1]. Extraction and separation of metal ions at low concentration using SLMs have been intensively studied during the last decade[2-4] .Under the assumptions of steady state, linear concentration gradients, very low value of the ratio Kds/KdF, instantaneous interfacial chemical reactions between metal species and the carrier, and low metal concentration, the following equation was derived for metal transport through a flat-sheet SLM[5,6] :

$$\ln \frac{C_F}{C_{OF}} = -\frac{S}{V_F} P\, t \text{.....(1)}$$

In a time interval, during which we have CF/COF >> KdS/KdS ,then the left-hand term in Eq. (1) deviates from linearity and, taking into account that in systems with SLM,

$$V_M / V_F \to 0$$

it approaches to a limiting value[2],

$$\ln\left\{\frac{C_F}{C_{OF}}\right\} = \frac{K_{ds} V_F}{K_{ds} V_F + K_{dF} V_S} \text{.....(2)} \qquad t \to \infty$$

Where:
t is the time in sec elapsed since the beginning of the permeation process. CF and CoF are the metal ion concentration at time t and zero time respectively.Kds and kdF are the distribution ratios of metal species between the membrane, the strip and the feed solution. V_F is the feed volume (cm3). *S* is the effective membrane area (cm2). P is the permeability coefficient (cm/s).

Published By:
Blue Eyes Intelligence Engineering
& Sciences Publication Pvt. Ltd.

II. EXPERIMENTAL

2.1. Preparation of nano crystallite hydroxyapatite (HAp). (N.el-said)

The synthetic hydroxyapatite (HAp) nanopowders were synthesized by chemical precipitation method. The procedure employed for the synthesis of HAp is as follows and all reagents were analytical grade, First, 0.5M $Ca(NO3)_2$ solutions and 0.3M$(NH_4)_2HPO_4$ solutions were obtained by dissolving $Ca(NO_3)_2 \cdot 4H_2O$ and $(NH_4)_2HPO_4$ in distilled water, respectively, and the pH of both solutions was adjusted to 11.0 by adding ammonia solution. The reactant molar ratio of Ca/P was kept at 1.667. The solution of $(NH_4)_2HPO_4$ was drop wisely added into the $Ca(NO_3)_2$ solution, and the white suspension was obtained. During the addition, the pH of the suspension was maintained at 11.0 using ammonia solution. After the complete addition, the suspension was further stirred for 24 h. Then the obtained suspension was filtrated and washed with distilled water and anhydrous ethanol for three times. The resultant powders were dried at 100 ^{0}C for 24 h, and then it was weighed and stored in tight glass container.

2.3. Preparation of Activated carbon (ACs).

Activated carbon, AC, was obtained from air-dried and crushed the date frond, DF. The raw material was inserted into a stainless steel tube fitted with an internal wire diaphragm and held in a vertical position to dispose of the formed tarry matter. Carbon was prepared by impregnating of the precursor with H_3PO_4 (50 vol%) followed by thermal treatment at 500 ^{o}C for two hours. The cooled activated mass was subjected to through washing with distilled water, so as get rid of extra acid and to attain pH values ≥ 6.5 in the washing solution, and finally dried at 110 ^{o}C

2.4. Radioactive tracers

The radioactive isotopes used in the present study were ^{137}Cs, ^{90}Sr, 60Coand $^{152+154}$Eu . All these isotopes were obtained from Amersham (England).All the pH values measured during the course of this work were accurately determined by employing a pH-meter of type B-417 HANA instrument. For equilibrium experiments a good shaker of the type SANKYO, a Centrifuge of the type UNIVERSAL with. a muffle furnace from LINDBERG and a special micropipette with disposable tips were used. Tri-Carb 1600 CA liquid scintillation analyzer was used for the determination of β-emission via liquid scintillation solution (Hionic fluxar) .Amodel 800A multichannel analyzer consisting of NaI(Ti) activated crystal flat type of 256 channels connected to an automatic scalar was used for counting the gamma activity.

2.5. Characterization of HAp-C.

This was achieved by the standard adsorption of N_2 at 77k, using a sorpatometer of the type NOVA 1000e (Quantachrome). In spite of limitations of the BET method, in case of activated carbon, it has been and will continue to be used for microporous adsorbents owing to its simplicity and reasonable [7]. Accordingly, the adsorption isotherms were analyzed to get various porous parameters: By applying the BET-equation to determine the S_{BET} surface area, total pore volume (V_P), from amount of nitrogen held at P/P^0 =0.95, and average pore dimension (radius) from $R=2V_P/ S_{BET}$ was evaluated. Other porous characteristics were estimated from the t-plots constructed by plotting volume of gas adsorbed (V_a) versus t-values of adsorption on non-porous standard carbon as reported by Selles-Perez and Martin-Martinez [18]. The obtained α_s-values were transformed into t-values by multiplication with 1.52 x 3.54 (Å) as suggested by the same authors. The following porosity characteristics were calculated as follows: total surface area (S_t) from slope of early straight line to zero, non-microporous surface area (S_n) from slope of the late straight portion, ultra micropore volume (V_{0u}) from early intercept of the base straight portion, and super micropore volume (V_{os}) from the late intercept of the base straight portion with V-axis.

2.6. Preparation of Nanoapatite disc

After preparation nanoapatite as nature bone with activated carbon were mixed together in a mortar. Subsequently,. The nanoapatite sample was prepared by stirring a sample of the ground mixture (g) in $CaCO_3$.$2H_2O$ aqueous solution (2.5 M, 100 mL,) at 80 °C for 1.0 hour under suitable conditions[19]. Similarly, the disc from nano mixtures-doped sample was prepared by stirring a sample of the ground mixture (10.0 g) in aqueous $CaCl_2$ solution for 1.0 hour at room temperature. Subsequently, the solid was filtered and dried at 100 °C under vacuum for 2.0 hours. And it was then re-suspended in de-ionized water (5–7 mL) to form thick paste that was placed in a metal mold (cylindrical aluminum mold with inner diameter of 20.0 mm) and pressed under The discs were first dried at 110 °C for 2 hours and then heated at 900 °C for 5-hours. Finally they were sintered 6 hours. From Aldrich, ^{60}Co in chloride media 99% from Merck. Other chemicals are analytical grade from Fluka Scientific. All chemicals and reagents used were of AR graded. The UV–VIS spectrum of the prepared solutions was determined using a Shimadzu UV–VIS recording spectrophotometer type UV-160 A. ^{137}Cs ,^{90} Sr and ^{60}Co in 0.5M HNO_3 was measured at λ=280nm,. An apparatus for membrane extraction in Fig. 1 was composed of two compartments vessels made of Teflon and Plexiglass and arranged both coaxially and horizontally. The liquid membrane was fixed on Sartorius SM cellulose nitrate micro porous carrier (thickness 65 ~m, diameter of pores 0.2 ~m, porosity 70%, effective area 6.25 cm^2) and placed at the bottom of the inner vessel.

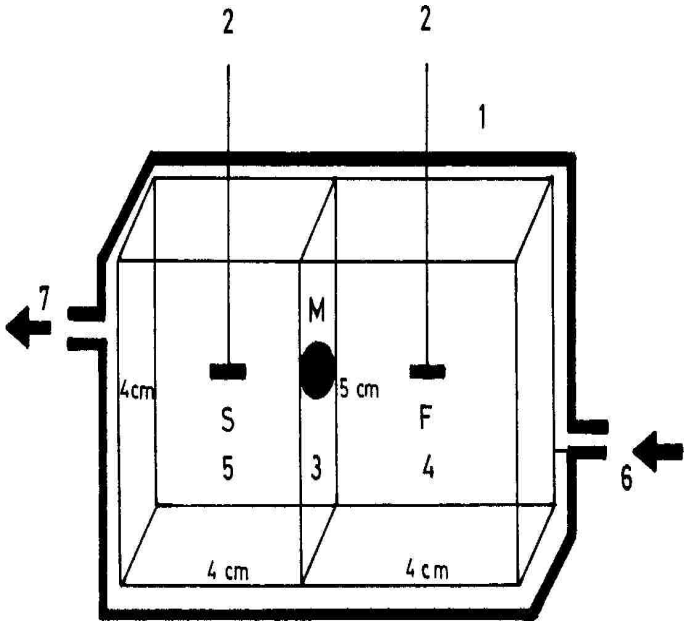

Fig. (1): Experimental installation of SLM process Characterization of Prepared Disc

Published By:
Blue Eyes Intelligence Engineering
& Sciences Publication Pvt. Ltd.

III. RESULTS AND DISCUSSION

3.1. Fourier Transform Infrared Spectroscopy (FTIR) analysis

The FTIR spectra can provide valuable information about the chemical compositions of the materials. Figure 2 shows the comparison FTIR spectra of raw date frond (Raw-DF), AC of date frond at 60% concentration of H_3PO_4 (AC-60%) and commercial activated carbon (AC-C) for comparison. Raw date frond (DF) in Figure 2 shows the most complicated and apparent spectrum. A strong and broad adsorption peak appeared at 3434.06 cm-1, which corresponds to the stretching of O –H functional and this shows the presence of bonded hydroxide in the raw sample. There was another peak group observed at 2930.44 cm-1 corresponding to the C–H sp3 stretching. A strong conjugated C=C peak also observed around 1633.83 – 1638.32 cm-1. This sample also shows four important absorption peaks at 1251.06, 1160.53, 1113.89 and 1053.53 cm-1 respectively which represent the stretching of C – O functional group. It can be suggested from 27 the spectrum that the main oxygen groups present in the raw-DF are carbonyl, ethers and alcohols group which are normally present in plant cellulose. In contrast to the FTIR spectrum shown by raw -DF, the spectrum AC-60% and AC-C illustrate less absorption peaks clearly, most of the absorption peaks of functional groups were diminished. Basically all the samples show a weak broad peak around 3425.12 –3440.32 cm-1, which indicates the presence of OH in the samples. It is most probably of the R-OH bonded like molecule in carbon. Finally, the spectra for the prepared activated carbon from date's frond chemical activated at 60% H_3PO_4 when comparable to the commercial AC, there seem a great similarity. This might indicate that the prepared AC is of similar in grade and standard of that the commercial prepared carbon.

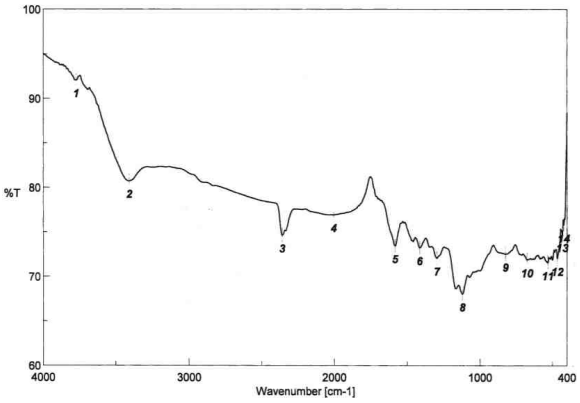

Fig(2): FTIR-Spectra for the synthetic HAp mixed with 40% DF carbon

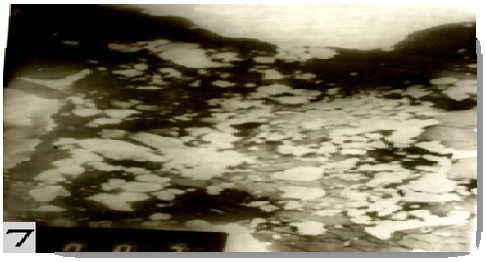

Fig(3): SEM Mixed with 40% of DF carbon for synthetic synthetic HAp

3.2. SEM micrographs

It provides information on the structural changes in the palm date frond for analysis during the activation process. Fig(3): SEM Mixed with 40% of DF carbon for synthetic HAp Figure 3 shows the micrograph of R-PDF at 500x magnification. The surface of R-PDF is curly form resulted from the presence of cellulose, hemicelluloses and lignin in the raw material without any cracks. This would account for its poor or negligible BET surface area.

3.3. Thermogravimetric analysis of date fronds

Figure 4 is the percentage weight loss during TGA for palm dates frond. Two major weights lost that took place in this graph. The first range of decomposition happened at 40 to 132 °C, which represent 6.1% weight lost. This is most possibly due to the moisture released by the sample during heating. The largest weight loss occurred at temperature range of about 132 to 400 °C. This is due to decomposition of chemical the high thermal stability.

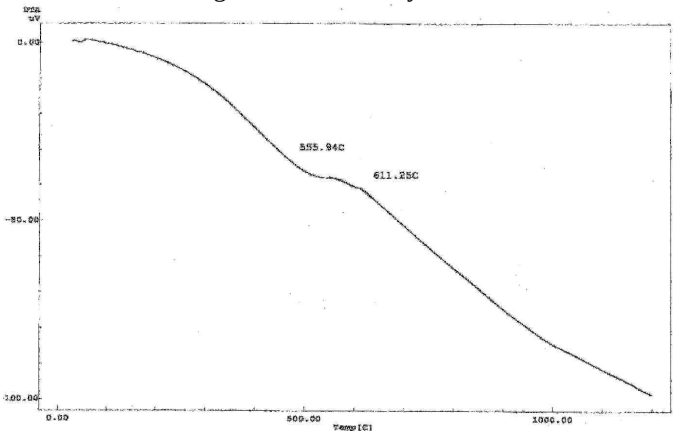

Fig (4): TGA-Spectra for SB mixed with 40% DF carbon

3.4. Single point BET Surface Area of Activated Carbon

The single point BET surface area analysis was done to study the effect of different activation method on the surface area of carbon samples. All the data collected, including the raw-DF, AC-40% and AC-C presented. Raw DF gives only 4.6 m2g-1 of BET surface area and for AC-60% is 1139 m2g-1. Comparatively, the synthesized samples exhibit slightly higher surface area than the commercial activated carbon which only 1069 m2g-1. This result proposed that the chemical activating agent used, H_3PO_4 has contributed to the higher surface area as compared to the commercial activated carbon.

3.5. Study the Permeation of 137Cs, 90,Sr and 60Co across through apatite disc / Activated Carbon (AC).

The mass transfer of ^{137}Cs, ^{90}Sr and ^{60}Co across the membrane is described in by considering only diffusion parameters. Figures(5-7) :Show the interfacial flux due to the chemical reaction is neglected, as the chemical reactions seem to take place at the interface aqueous source solution-membrane , membrane-receiving aqueous solution interfaces, and different studies suggest that chemical reactions can be considered as occurring instantaneously relative to the diffusion process. Therefore, to model the mass transfer of ^{137}Cs, ^{90}Sr and ^{60}Co, it is necessary to consider diffusion of the solute through the aqueous source boundary layer, the reversible chemical reaction at the interface and diffusion of the metal complex species in the

Published By:
Blue Eyes Intelligence Engineering
& Sciences Publication Pvt. Ltd.

membrane. Membrane permeability's were determined by monitoring metal on centration UV-Perkin Elmer 1100B spectrophotometer in the source phase as a function of time. The permeation coefficient *P* was computed by equation(1) . The permeation of ^{137}Cs, ^{90},Sr and ^{60}Co through supported liquid membrane solution(SLMs) (nano apatite disc), containing H(suitable membrane for radioactive tracers as carrier was also studied. From the detailed study of the permeation process through dsic SLMs as function of aqueous pH, membrane carrier concentration and stirring rate of the aqueous solutions.

3.6. Effect of Extraction equilibrium

The transport of ^{137}Cs, ^{90,Sr} and ^{60}Co through disc - supported liquid membrane containing Alamine336 diluted in toluene impergenated was examined. The mass transfer rate, expressed as permeability, P, focused on diffusion through the aqueous layer in the feed solution, the organic layer and the aqueous layer in the stripping solution. The aqueous feed solution speed homogenizer (300-800 ml/min), carrier concentration (0.1-20% v/v), aqueous stripping solution homogenizer (300-1300 ml/min) and feed concentration 1250 ppm) with 0.5 M HNO_3 in the product phase. pH of the feed solution was 5.0. The measured permeabilities were compared to generally accept mass transfer correlations. The validity of the prediction was evaluated with the experimental data, and the data were found to tie in well with the theoretical values.

$$U = \Sigma(\log D_{cal} - \log D_{\exp})^2 \text{.....(3)}$$

Where D_{exp} = experimental values of the distribution coefficient and D_{cal} are the corresponding calculated values from the relevant mass balance equation for a proposed model. Results obtained from the numerical treatment showed that the extraction of ^{137}Cs ,^{90},Sr and ^{60}Co is best represented by:

$$H^+_{aq}X(OH)_2(NO)_3^- + \overline{2L} + HCs(OH)_2(NO)_3^- \overline{L}_2 \text{.....(4)}$$

Where L is represents the ligand. The value of *K Equ.5*.
X is ^{137}Cs,^{90},Sr and ^{60}Co

$$K_{ext} = \frac{\overline{[HX(OH)_2(NO)_3L]}}{[H^+]_2[X(OH)_2(NO)_3^-]_{aq}\overline{[L]^2}_{i,r}} \text{.....(5)}$$

3.7. The permeation model

The permeation of ^{137}Cs,^{90},Sr and ^{60}Co through disc supported liquid membranes (SLMs) impregnated with Alamine336 diluted in toluene has been investigated. A model is reported describing in Figures(11-13).The transport mechanism which consists of: diffusion process through the feed aqueous diffusion layer, permeation factor for disc supported liquid membrane fast interfacial chemical reaction and diffusion through the membrane. The experimental data are quantitatively explained by mathematical equations describing the rate of transport. Different rate-controlling processes take place as long as the metal transport occurs. The $^{152+154}Eu$ transport rate is determined by the rate of diffusion of ^{137}Cs, ^{90,Sr} and ^{60}Co. The rate of diffusion through the disc supported liquid membrane. Then, the adsorbed of ^{137}Cs,^{90},Sr and ^{60}Co crossing the membrane may be derived by applying Fick's first diffusion law to the diffusion layer on the source side, and to the membrane. The diffusional adsorption and the source aqueous boundary layer *J* and at the membrane *J* can be expressed as org. by the following equations: □

$$J_m = \Delta m^{-1}([X(n)])_{TOT} - [X(n)_{i,TOT}) \text{.....5}$$

$$J_{org} = \Delta_{org}^{-1}[HX(III)(OH)_2(NO)_2^-\overline{L}_2]_{i-s} - [HX(OH)_2CL_2^-L_{2org}]_{i,r} \text{.....6}$$

The distribution coefficient of ^{137}Cs ,^{90}Sr and ^{60}Co between the membrane phase and the receiving phase is much lower than that between the source phase and the membrane, the concentration of the ^{137}Cs ,^{90}Sr and ^{60}Co extracted complex in the membrane phase on the receiving solution side may be negligible compared with that on the source solution side.

$$J = \Delta^{-1}([HX)(n)(NO).L_2]_{i,s} \text{..... ....7}$$

If the chemical reaction in equation 3 assumed fast reaction if compared to the diffusion rate, local equilibrium at the interface is reached and concentrations at the interface are related through the expression equation 8.

$$K_{ext} = \frac{\overline{[[HX(n)(OH)(NO)_3.\overline{L_2}]]}}{([H^+]_{aq}[(X(u)(OH)_2(NO)I_2^-]_{aq}[L]^2_{org}]_{i,r}} \text{...}$$

.....8

Where the steady state, $J_s=J_{org}=J$

$$J_{ext} = \frac{K_{ext}[H^+][L]^2}{\Delta_{org} + \Delta_{as}K_{ext}[H^+][L]^2}[X(n)I)_{TOT} \text{.....9}$$

The permeability coefficient can be defined as:

$$P = \frac{K_{ext}[H^+][L]^2}{\Delta_{org} + \Delta_{as}K_{ext}[H^+][L]^2}[X(m)_{TOT} \text{.....10}$$

3.8. Effect of pH on feed phase.

The Effect of the feed solution acidity at varying pH ≈0.1-0.5M HNO_4 on the transport of ^{137}Cs ,^{90}Sr and ^{60}Co was studied In Figs(5-7). The initial metal concentration in the feed was 0.05M much lower than the carrier concentrations. A solution of 0.05M EDTA was used as the stripping phase. The distribution of the ^{137}Cs,^{90},Sr and ^{60}Co species as a function of solution pH transport of ^{137}Cs, in all systems through disc membrane investigated can be described by reaction mechanism and study the time interval from 0.5 to 1 h and feed metal concentration CF_D 0.01M, when $[HNO_3]_{0F}$ 0.1M and the feed acidity decreased to pH ≈4.9, the HNO_3 transport from the feed into the strip solution decreased. It Shows the permeability coefficients of the metal of feed against permeability show figure (8-10) . Consequently, the acid concentration gradient in the feed diffusion layer decreased due to the transport of HCl and caused an increase of K_{dF} of ^{137}Cs. On the other hand, an increase in K_{dS} ^{137}Cs can be demonstrated at pH 0.1-6.8, in consequence of increasing significance of the solvation mechanism through disc membrane. And the effects led to the decrease of P_F of Cesium^{137}at $[HCl]]_F$

Published By:
Blue Eyes Intelligence Engineering
& Sciences Publication Pvt. Ltd.

0.1M where K_{dS} decreases rapidly with increasing $[HNO_3]_F$. Where V is the volume of HNO_3 of the feed phase solution, A is the effective membrane area, $[M]_0$ and $[M]_t$ are the concentrations of metal in the feed phase at time zero and at a given time, and t is the elapsed time. It can be point out that the above expression was obtained under condition of the fully intermix in the feed chamber. The Permeability of ^{137}Cs depends on membrane solubility and the presence of specific integral transport radioactive. Other factors such as pressure, concentration, and temperature of the molecules or solutes on either side, as well as the size of the molecules can also affect permeability. Permeability at higher carrier concentrations. This constant permeation coefficient value, or limiting permeability (P_{lim}), can be attributed to the assumption that diffusion in the membrane is negligible compared with the aqueous diffusion and the permeation process is controlled by the diffusion in the stagnant film of the feed phase. Thus the maximum permeability were found to be (9,7,3)x10^6 cm/sec for ^{90}Sr , ^{60}Co and ^{137}Cs ,respectively.:

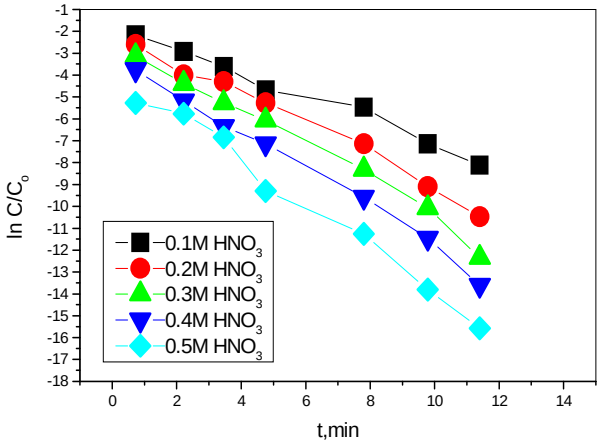

Fig.5.Effect of pH on feed phase.Plot of ln C_F/C_o against t, min for permeation of Cs(137),F=xM $NaNa_3$,pH=0.1 HNO_3 ,HA-AC=0.1M/xylene,S=0.015 EDTA.

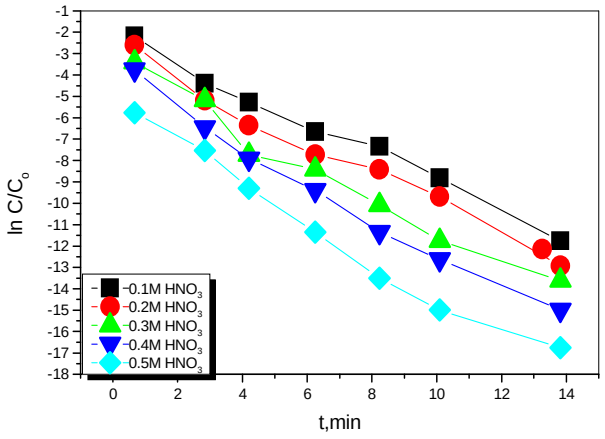

Fig.6.Effect of pH on feed phase.Plot of ln C_F/C_o against t, min for permeation of Sr(90),F=xM $NaNa_3$,pH=0.1 HNO_3 ,HA-AC=0.1M/xylene,S=0.015 EDTA.

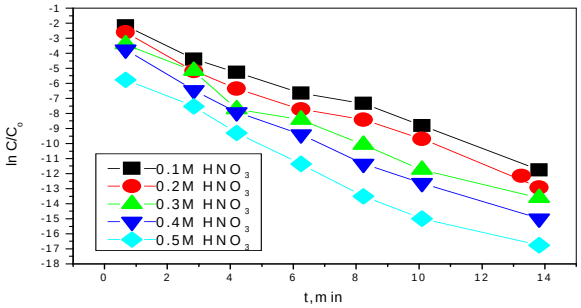

Fig.7.Effect of pH on feed phase. Plot of ln C_F/C_o against t, min for permeation of Co(60),F=xM $NaNa_3$,pH=0.1 HNO_3, HA-AC=0.1M/xylene,S=0.015 EDTA.

$$P_{\lim} = \frac{D_{aq}}{d_{aq}} = 9x\times10^{-6}\, cm/s \text{.....(11)}$$

And assuming a value of 10^{-5} cm^2/s for D_{aq} (average diffusion coefficient), then d_{aq}= 7.44x10^{-3} cm. This value (d_{aq}) is the minimum thickness of the disc apatite an aqueous diffusion layer in the present experimental conditions. The Effect of the feed solution acidity at varying pH ≈0.1-4.2 on the transport of ^{90}Sr. Fig (6) was studied. The initial metal concentration in the feed was 0.05M much lower than the carrier concentrations (0.25M). A solution of 0.05M EDTA was used as the stripping phase.

3.9: Effect of feeding phase concentration

Effect of on transport ^{137}Cs, ^{90,Sr} and ^{60}Co from nitrate media was studied . The supported liquid membrane of ^{137}Cs,^{90},Sr and ^{60}Co from sodium nitrate solutions by n-HA-AC was also studied previously. in Fig's (8-10) The extraction equilibrium is described by the next general following reaction:

$$H^+_{aq} + X[(NO_3)]^-_4 + nL_{org} \Leftrightarrow X[(NO_3)]^-_4 + nL_{org} \ldots 13$$

Where L is the organic extractant and n represented a stoichiometric coefficient. Thus, from 0.1 M HNO_3 concentration in the aqueous media, the maximum permeability was found to be for ^{137}Cs,^{90},Sr and ^{60}Co from nitrate media. Thus the maximum permeability were found to be (10,8,4)x10^6 cm/sec for ^{90}Sr , ^{60}Co and ^{137}Cs (Fig.21) ,respectively.:

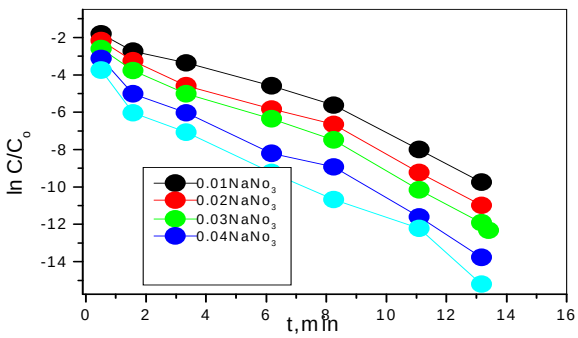

Fig.8.Effect of feeding phase concentration .Plot of ln C_F/C_o against t,min for permeation of Cs(137),F=xM $NaNa_3$,pH=0.1 HNO_3,HA-AC=0.1M/xylene,S=0.015 EDTA.

Published By:
Blue Eyes Intelligence Engineering
& Sciences Publication Pvt. Ltd.

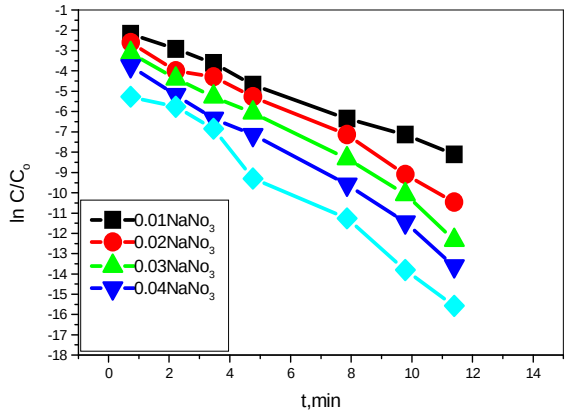

Fig.9.Effect of feeding phase concentration .Plot of ln C_F/C_o against t,min for permeation of Sr(96),F=xM $NaNa_3$,pH=0.1 HNO_3,HA-AC=0.1M/xylene,S=0.015 EDTA.

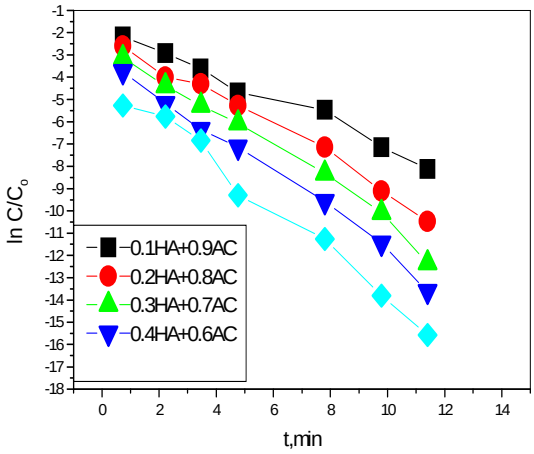

Fig.11.Effect of carrier concentration on the permeability Plot of ln C_F/C_o against t,min for permeation of Cs(137),F=xM $NaNa_3$,pH=0.1 HNO_3 HA-AC=0.1M/xylene,S=0.015 EDTA.

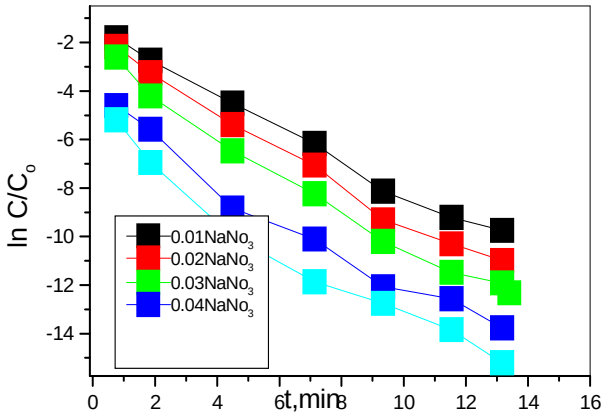

Fig.10.Effect of feeding phase concentration .Plot of ln C_F/C_o against t,min for permeation of ^{60}Co,F=xM $NaNa_3$,pH=0.1 HNO_3,HA-AC=0.1M/xylene,S=0.015 EDTA.

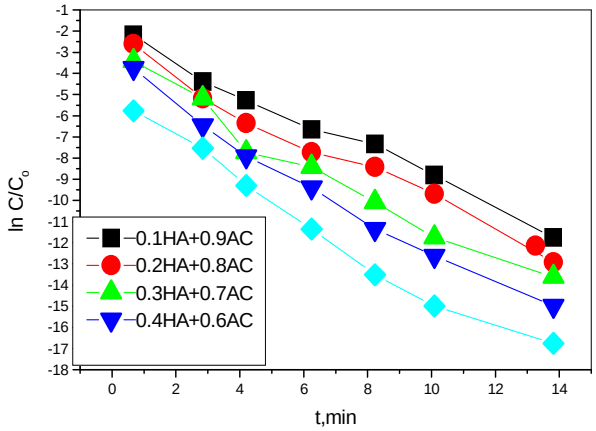

Fig.12.Effect of carrier concentration on the permeability Plot of ln C_F/C_o against t,min for permeation of Sr(90),F=xM $NaNa_3$,pH=0.1 HNO_3,HA-AC=0.1M/xylene,S=0.015 EDTA.

3.9. Effect of carrier concentration on the permeability of 137Cs, 90Sr and 60Co

The results concerning transport of radioactive isotopes from a feed phase containing 3.5×10^{-5} M ^{137}Cs,^{90}Sr and ^{60}Co in 5 M HNO_3, Fig(11-13). The receiving phase being another radioactive waste , and varying concentrations of HAP composite in the range 0.1 to 0.7 M dissolved in toluene on disc hydroxyapatite support, revealed no change in the permeation coefficient (5.2×10^{-3} cm/s) at higher carrier concentrations (0.1-0.9 M) against the value of 2.9×10^{-3} cm/s obtained for a 0.22 M HAP composite solution in toluene. Accordingly to Eq (12) and considering the value of 4×10^{-3} cm/s as the limiting permeability value, the thickness of the aqueous diffusion film is calculated as 2.8×10^{-3} cm.

$$P_{\lim} = \frac{D_{aq}}{d_{aq}} = 1.9\times10^{-3}\, cm/S \quad \text{.....(12)}$$

and assuming a value of 10^{-5} cm^2/s for D_{aq} (average diffusion coefficient) , then $d_{aq}= 5.3\times10^{-3}$ cm. This value (d_{aq}) is the minimum thickness of the disc apatite in aqueous diffusion layer in the present experimental conditions. Thus the maximum permeability were found to be $(12,8.5,5)\times10^6$ cm/sec for ^{90}Sr , ^{60}Co and ^{137}Cs ,respectively.:

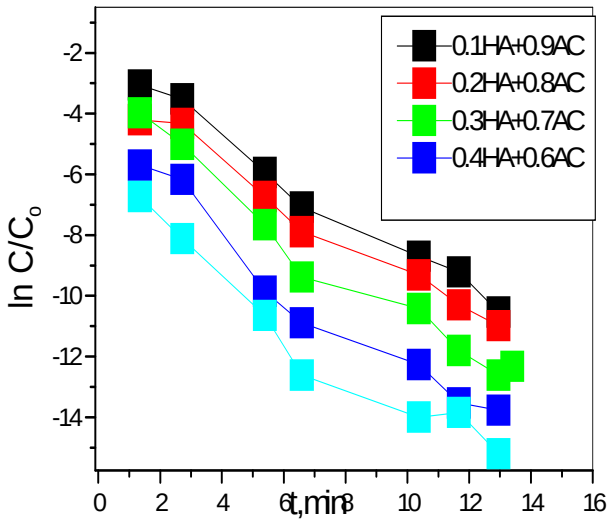

Fig.13.Effect of carrier concentration on the permeability Plot of ln C_F/C_o against t,min for permeation of Co(60),F=xM $NaNa_3$,pH=0.1 HNO_3,HA-AC=0.1M/xylene,S=0.015 EDTA.

Published By:
Blue Eyes Intelligence Engineering
& Sciences Publication Pvt. Ltd.

3.10. Effect of stripping concentration.

Effect of stripping phase (EDTA) on transport of ^{137}Cs,^{90},Sr and ^{60}Co from nitrate media was studied The supported liquid membrane of ^{137}Cs,^{90},Sr and ^{60}Co from sodium nitrate solutions by alamine 336/toluene was also studied previously.Fig's (14-16) The extraction equilibrium is described by the next general following reaction:

$$H^{+}_{aq} + X[(NO_3)]^{-}_4 + nL_{org} \Leftrightarrow X[(NO_3)]^{-}_4 + nL_{org} \ldots\ldots 13$$

Where L is the organic extractant and n represented a stoichiometric coefficient. Thus, from 0.1 M HNO_3 concentration in the aqueous media, Thus the maximum permeability were found to be (13,11,63)x10^6 cm/sec for ^{90}Sr , ^{60}Co and ^{137}Cs ,respectively.

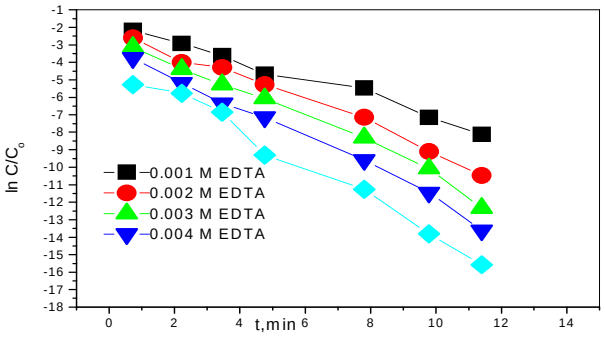

Fig.14.Effect of stripping concentration.Plot of ln C_F/C_o against t,min for permeation of Cs(137),F=0.05M $NaNa_3$,HA-AC= XM/xylene.

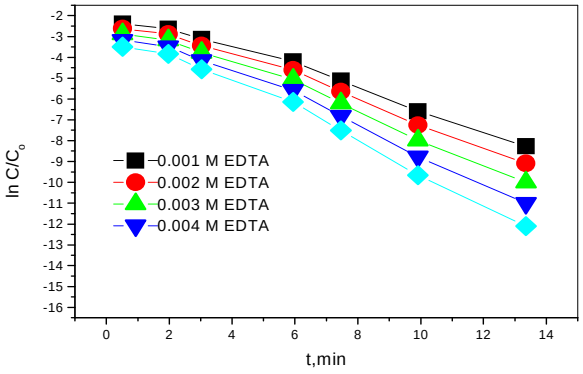

Fig.15.Effect of stripping concentration.Plot of ln C_F/C_o against t,min for permeation of Sr(90),F=0.05M $NaNa_3$,HA-AC= XM/xylene.

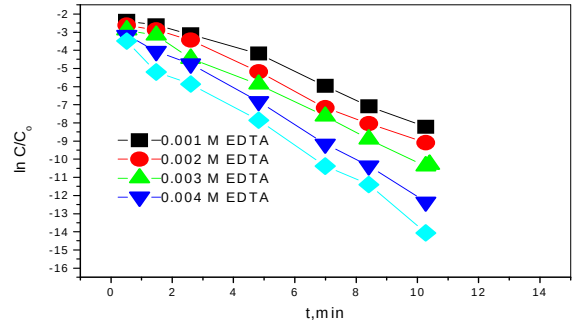

Fig.16.Effect of stripping concentration.Plot of ln C_F/C_o against t,min for permeation of Co(60),F=0.05M $NaNa_3$,HA-AC= XM/xylene.

IV. EFFECT OF TEMPERATURE

Increase in the permeability coefficient by increasing temperature up to 298 K. At fixed stirring rate, (Fig 17), the natural logarithm of the rate constant was found to be linear with respect to 1/*T* which allowed estimating the activation energy of the slope of the straight line according to the Arrhenius and Eyring equations. The activation energies from temperature range 278–298K for the studied system was calculated to be 15.45 , 18.523.12, k cal/mol at our hydrodynamic conditions.

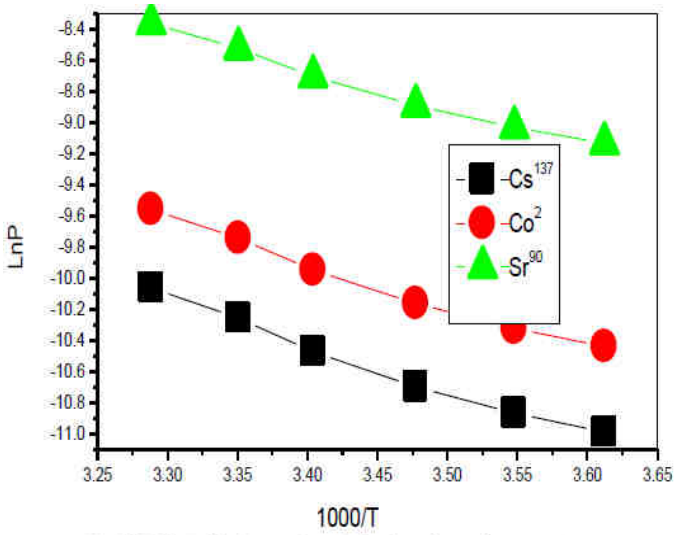

Fig(17):Plot of ln P against t,min for effect of temperature on the radioactive isotopes,F=0.05M $NaNa_3$,HA-AC=XM/xylene.

The estimated activation energy falls in the suggestion that the transport of ^{137}Cs,^{90},Sr and ^{60}Co is likely controlled by chemical reaction controlled process**.** Show the Table.1. Depicts the maxnium permeability coefficient for at theses hydrodynamic conditions conditions. Table(2): The reproducibility of permeability as a function of repeating times in Table.2.Permeability coefficient in terms of reproducibility at interval (*P*=106 m/s) of feed (*P*=1x10-^{6} m/s) of strip for ^{137}Cs, ^{90}Sr and ^{60}Co.

Table.1. Depicts the maxnium permeability coefficient for at theses hydrodynamic conditions conditions

Px10^6			
	Sr(90)	Co(60)	Cs(137)
Feed	10.25	9.7	2
membrane	0.45	0.275	0.33
strip	425	222	175

The reproducibility of permeability as a function of repeating times in Table.2.

Published By:
Blue Eyes Intelligence Engineering
& Sciences Publication Pvt. Ltd.

Table.2.Permeability coefficient in terms of reproducibility at interval (P=106 m/s) of feed (P=1x10^{-6} m/s) of strip for ^{137}Cs, ^{90}Sr and ^{60}Co.

1 (P=1x10^{-6} m/s), ^{137}Cs		(P=1x10^{-7} m/s), ^{90}Sr		(P=1x10^{-8} m/s), ^{60}Co	
	After	Before	After	Before	After	Before
1	156±0.8	160.9±0.3	144±0.8	160.9±0.3	144±0.8	1160.9±0.3
2	215±0.31	220.8±0.25	215±0.31	220.8±0.25	215±0.31	220.8±0.25
3	239±0.8	241±0.3	250±0.8	241±0.3	250±0.8	241±0.3
4	2600±0.7	252.5±0.4	2600±0.7	252.5±0.4	2600±0.7	252.5±0.4
5	270±0.45	261.90 ±.5	270±0.45	261.90 ±.5	270±0.45	261.90 ±.5
6	280±0.62	316.8±_0.65	280±0.62	316.8±_0.65	280±0.62	316.8±0.65
7	290±0.4	315.7_±0.32	290±0.4	315.7_±0.32	290±0.4	315.7±0.32
8	2840.35	275±0.28	2840.35	275±0.28	2840.35	275±0.28
9	274±0.	35 29.5±0.39	274±0.	35 29.5±0.39	274±0.	35 29.5±0.39
10	280.31	277.4±0.45	280.31	277.4±0.45	280.31	277.4±0.45

V. CONCLUSIONS

The transport of ^{137}Cs ,^{90}Sr and ^{60}Co using the hydroxyapatiteA.C composite various experimental conditions has been studied and a mechanism of ^{137}Cs ,^{90}Sr and ^{60}Co transport considering the aqueous film diffusion of metal ions, fast chemical reaction at the interface and diffusion of ^{137}Cs ,^{90}Sr and ^{60}Co through the membrane is proposed. For concentrations of HAP higher than 0.30 M, a limiting value of 0.3M for permeability is obtained and the transport process is controlled by the diffusion in the aqueous stagnant film. .The separation of ^{137}Cs, ^{90}Sr and ^{60}Co can be was a chievied by HA/AC using EDTA solutions by a supported liquid membrane .The activation energies from temperature range 278–298K for the studied system was calculated to be 15.45 , 18.523.12, , k cal/mol at our hydrodynamic conditions. The estimated activation energy falls in the suggestion that the transport of ^{137}Cs ,^{90}Sr and ^{60}Co is likely controlled by chemical reaction controlled process.

The nHA-AC shows favorable carrier membrane with higher surface area to ^{90} Sr> ^{60}Co> ^{137}Cs**.**The nHA-AC can be used in medical and technological applications.that of bone material. Porous HA ceramics have found enormous use in biomedical applications including bone tissue regeneration, cell proliferation, and drug delivery. In bone tissue engineering it has been applied as filling material for bone defects and augmentation, artificial bone graft material, and prosthesis revision surgery. Its high surface area leads to excellent osteoconductivity and restorability providing fast bone in growth Hydroxyapatite is the most widely accepted biomaterial for the repair and reconstruction of bone tissue defects. It has all the characteristic features of biomaterials, such as, biocompatible, bioactive, osteoconductive, non-toxic, non-inflammatory and non-immunogenic properties

REFERENCES

[1] Xu, H. H, Simon,C. G., 2004. surface textures as potential .*J. Biomed Mater Res* ***A*** .69, 267-78

[2] Xu, H. H, and Simon, C. G.,2004. Development of new approaches to the treatment. *J. Orthop Res*. 22, 535-43.

[3] Yang, Y. Z, Tian ,J. M. Morphological behavior of osteoblast-like.,2002. *J. Bio.materials* . 23, 1383-89.

[4] Yoshimura, M, Ioku, K. **1993**. Apatite whisker and method for preparation "US Patent and Trademark Office.,5,227-237.

[5] Yuasa, T, Miyamoto, 2004.Y. Smart nanoprobes for the detection *J. Biomaterials*., 25, 1159-66.

[6] Yubao, L, Groot, K. A review of preparation methodologies.1994.*J .Mater Sci Mater Med*., 5, 326-31.

[7] Torricelli, P, Fini, M. interaction between tenocytes .*2003.J. Biotechnol* .,31, 263-77.

[8] Trail, I. A., Martin, J. A. This versatile model allows for evaluation.2004. *J. Bone Joint Surg* Br .,86, 1002-6.

[9] USDHHS, A. Report of the Surgeon General. Rockville, MD, USDHHS, Office of the Surgeon General**. 1999.**

[10] Vallet-Regi, Ramila,M. A. silica-based ceramics receive a great interest. *2004.J . Biom. Mate. Res A.*, 66, 580-5.

[11] 11-Van Nausdle, J. A. The role of a Catholic.2005. *J. University of Notre Dame*, 46556-64.

[12] Vignesh, R. C., Sitta, Djody.S. proliferation, differentiation, mineralization and cyto-*toxicity*.2006. *J. Toxicology*., 220, 63-70.

[13] Wang, C., Duan, Y. *J. Biomaterials* .**2004**,25, 2507-14.

[14] Wei, G; Ma ,P. X. Biomimetic nanofibrous scaffolds for bone tissue.2005.*J. Biomaterials*, 25, 4749-57.

[15] Wenk, H. R, Heidelbach, F. 1999.Crystal alignment of carbonated apatite in *bone* ..*J. Bone*., 24, 361-9.

[16] Roeder, R. K., Sproul ,M. M. properties compared to the use of an equiaxed powder.2003. *J .Bio. Mat. Res A*.,,67, 801-12.

[17] Kim, H. W., Knowles ,J. C. The function of terpene natural products in ..2005.*J .Bio. Mat. Res A* .,72, 258-68.

[18] El-Said, N.;Abdel rahman .N.; Ali ,M.S. *J. of Appl. Chem* (IOSR-JAC).**2014**,7, 103-111

Published By:
Blue Eyes Intelligence Engineering
& Sciences Publication Pvt. Ltd.